International Journal of Emerging Research in Management &Technology
ISSN: 2278-9359 (Volume-5, Issue-12)

Research Article | **December 2016**

DC Microgrid for Buildings Integrated Renewable Energy Sources

Duc Nguyen Huu, Hung Truong Nam*
Faculty of Energy Technology; Electric Power University,
Vietnam

Abstract—

Integration of wind and solar within dc microgrids into a so-call net zero-energy buildings is studied. The dc ring microgrid is proposed to include a wind energy conversion system (WECS), a photovoltaic array (PV) and battery energy storage system (BESS). First, an optimized operation strategy in day ahead is presented to utilize maximum clean energy and minimum consumption of electricity from the main grid. Optimal generated power operation of the WECS and PV is run follows on the maximal power point tracking method (MPPT). Second, a coordinated droop scheme is introduced to provide coordination control of BESS and the main AC grid. Several simulations are performed to realize the presented method.

Keywords— Net-zero building, Wind energy, Photovoltaic array, Battery Storage, Optimized operation, Droop control

I. NOMENCLATURE

T	Optimization time span in hours
$F(P_{dg}(t))$	Electricity cost function from the AC grid
c_{low}, c_{high},	Electricity price coefficients
$P_{AG}(t)$	Output power of the AC grid
$P_w(t)$	Output power of the wind energy conversion system
$P_{pv}(t)$	Output power of the PV modules
$P_b(t)$	Power exchange between the battery and the AC bus
$P_l(t)$	Demand power of loads
$P_{Renew}(t)$	Output power from renewable sources
P_{bmin}	Lower limit of the power of the battery
P_{bmax}	Upper limit of the power of the battery
P_{AGmin}	Lower limit of output power of the AC grid with AC/DC converter
P_{AGmax}	Upper limit of output power of the AC grid with AC/DC converter
$P_{min\text{-}AG}$	Lower limit of the output power of the AC grid concerning battery power exchanges
$P_{max\text{-}AG}$	Upper limit of the output power of the AC grid concerning battery power exchanges
DOD	Depth of discharge of the battery
E_b	Battery storage capacity
E_{b0}	State of the charge of the battery at the beginning of optimization
$P_{b\text{-}in}(t)$	Internal power of the battery
η_{dis}	Discharging efficiency of the battery
η_{ch}	Charging efficiency of the battery
E_{Res}	Amount of allocated reserves in the battery
ΔP_{Renew}	Hourly uncertainty of generation from renewable resources
ΔP_W	Hourly uncertainty of generation from the wind source
ΔP_{PV}	Hourly uncertainty of generation from PV arrays
ΔP_l	Hourly uncertainty generation from loads
ΔT_{Res}	Required time that the reserve has to be available

II. INTRODUCTION

Buildings play a significant role on energy consumption and the environment impact. In Vietnam, commercial and residential buildings use around 40% of the electricity. New buildings in urban, thus more energy used by buildings are increasing because of strong growth of Vietnam's economy. This can lead to install more thermal power plants, thereby making more issues on environmental as well as economical aspect. This challenge could be partly solved by integration of wind and solar into commercial buildings.

Concept of a net-energy building (ZEB) is introduced to harvest energy from wind and solar in urban areas. With ZEB, electricity consumption from the main grid can be reduced through the balance of generated clean energy with demand in buildings. Integration of wind and solar on a rooftop is studied in [1-3]. BESS are commonly adopted to overcome the uncertainty problem of renewable energy sources. The merits of the integration of BESSs with RES are reported in [7-9]. The operational strategy considering the economic cost and life time of battery storage in stand-alone hybrid system is presented in [10]. According to this strategy, the lifetime of battery storage is maximized by reducing operation mode change. The battery scheduling method that optimizes the usage of RES and makes the battery lifespan

© 2016, IJERMT All Rights Reserved

longer is introduced in [11]. In order to do this strategy, a programmable logic controller is used to control and monitor the communication among the components. The author of [10] proposes an operation strategy for the hybrid wind-battery system in order to minimize the electricity production cost while ensuring that the load is served according to a certain reliability criteria.

In buildings, DC grid is a good concept to integrate RES because of its inherent advantage for DC output voltage such as photovoltaic (PV) arrays, battery energy storage systems (BESS), DC loads in industrial and residential applications. In comparison with AC micro-grids, DC micro-grids can eliminate DC-AC or AC-DC power conversion stages of renewable sources and loads, therefore not only the size and cost of the DC system could be reduced but also its efficiency could be increased. For these above mentioned reasons, several studies have investigated the deployment of DC distribution networks [10-16].

In this paper, an optimized scheduling of a combined wind-solar system together with battery storage in commercial buildings is developed. The battery storage system is scheduled with objective of minimization of electricity consumption from the main grid. A share of energy capacity of the battery storage is allocated to deal with intermittency of the wind-solar generation and minimize usage of the grid. Therefore, positive and negative energy reserve is allocated in the battery. In addition, DC voltage is stabilized according to the dc droop control applied to resources. The dc droop control is implemented to coordinate between BESS and the AC grid.

The rest of this paper is organized as follows. Section 3 describes outline of the dc microgrid. Optimized operation strategy is introduced in section IV. A control system applied to the microgrid is presented in section V. Simulations are carried out to realize effectiveness of the presented method in section VI. The conclusions are drawn in section VII.

III. OUTLINE OF A DC RING MICROGRID FOR BUILDINGS

A schematic of the dc microgrid for buildings integrated renewable energy sources with the relevant power flows is shown in Figure 1. The microgrid is composed of a wind energy conversion system (WECS); a photovoltaic system (PV) and a battery energy storage system (BESS). Because wind and solar energy sources are stochastic, a battery energy system is therefore integrated into the system to reduce usage of electricity from main AC grid and thus reduce emission of the system and also minimize the operation cost. Other advantages that the battery can provide is load-frequency control, voltage control, providing reserve, capturing excess renewable generation and increasing the value of generated renewable energy by shifting the usage time in an economically optimized way. WECS is connected to the dc bus through an AC/DC converter. BESS is integrated to the dc bus via a bi-directional buck converter. PV is connected to the dc bus through an DC/DC converter. The WECS employs permanent magnet synchronous generator (PMSG). BESS of Vanadium Redox (VRB) is used because its power and capacity can be independently chosen. Therefore, the optimal capacity of BESS is designed. The dc microgrid is interconnected to the AC grid through a DC/AC converter and a transformer.

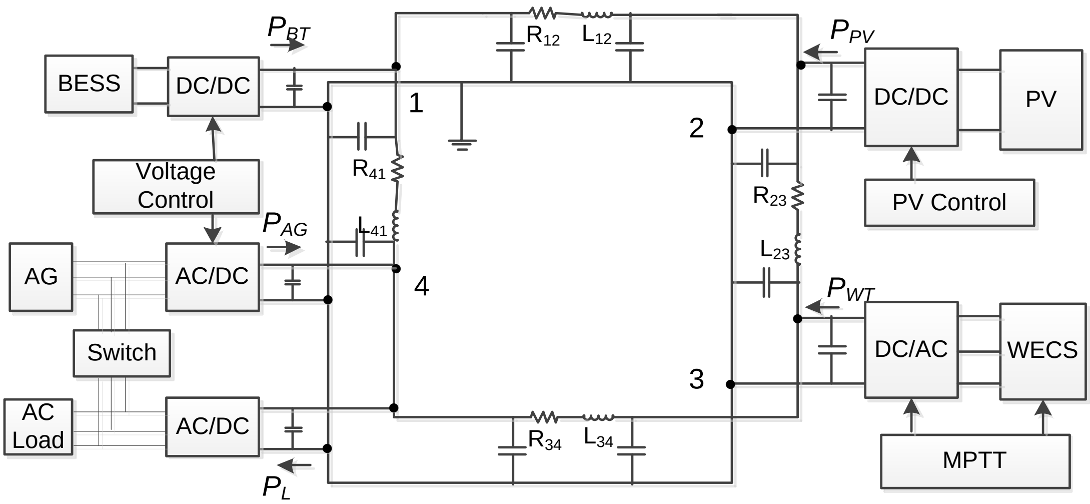

Fig. 1 Diagram of a dc ring microgrid in buildings integrated wind and solar

IV. OPTIMIZED OPERATION STRATEGY OF THE DC MICROGRID

A. Description of the method

The operation strategy of the dc microgrid is to utilize maximum possible clean energy from wind and solar, thus reduce the cost of operation and emission of the system via the battery scheduling. An optimized operation strategy is formulated and implemented in MATLAB optimization toolbox. The method is a nonlinear constrained optimization. It employs a sequential quadratic programming (SPQ) method. The following assumptions are used to formulate the problem:

- Forecasted power output of wind and solar generation is available for hourly intervals. Uncertainties of forecasts are also given in percentage of installed capacity.

- Forecasted load curve are known, and electricity prices for low and high demand hour are given also.
- The battery characteristics for example depth of discharge (DOD), power and energy capacity, charging and discharging efficiencies are known.

B. Optimization Formulation

The objective of the optimization is to utilize maximum renewable energy, thus minimization of the operational cost and emissions. Therefore, the objective function can be defined as follows:

$$\min(\sum_{t=1}^{T} F(P_{\mathrm{AG}}(t))) \tag{1}$$

Electricity cost function can be determined as follows:

$$F(P_{\mathrm{AG}}(t)) = \begin{cases} c_{low} P_{\mathrm{AG}}(t) & \text{in low demand hour} \\ c_{high} P_{\mathrm{AG}}(t) & \text{in high demand hour} \end{cases} \tag{2}$$

In other words, the energy from wind farm and photovoltaic is scheduled optimally with the help of the battery storage system. In this way, the electricity consumption from the main grid is minimized. As a result, the minimum operational cost of the system and amount of the emissions are determined. This objective function is subjected to the following constraints:

1) Equality constraint of load-generation from Fig. 1:

$$P_{\mathrm{w}}(t) + P_{\mathrm{pv}}(t) + P_{\mathrm{AG}}(t) + P_{\mathrm{b}}(t) - P_{\mathrm{l}}(t) = 0 \tag{3}$$

$$P_{\mathrm{Renew}}(t) = P_{\mathrm{W}}(t) + P_{\mathrm{pv}}(t) \tag{4}$$

Equation (3) is valid for all the scheduling time. P_b is bidirectional. If the battery is in charging mode the sign of power would be negative.

2) The exchange power between the battery and the DC bus can be defined as following:

$$P_{\mathrm{b}}(t) = -P_{\mathrm{Renew}}(t) - P_{\mathrm{AG}}(t) + P_{\mathrm{l}}(t) \tag{5}$$

The limitations of the battery power introduce a boundary constraint to the objective function:

$$P_{\mathrm{bmin}} \le P_{\mathrm{b}}(t) \le P_{\mathrm{bmax}} \tag{6}$$

By substituting (5) into (6):

$$P_{\mathrm{bmin}} \le -P_{\mathrm{Renew}}(t) - P_{\mathrm{AG}}(t) + P_{\mathrm{l}}(t) \le P_{\mathrm{bmax}} \tag{7}$$

This constraint can be translated to:

$$P_{\mathrm{AG}}(t) \le -P_{\mathrm{bmin}} - P_{\mathrm{Renew}}(t) + P_{\mathrm{l}}(t) \tag{8}$$

$$P_{\mathrm{AG}}(t) \ge -P_{\mathrm{bmax}} - P_{\mathrm{Renew}}(t) + P_{\mathrm{l}}(t) \tag{9}$$

3) By limiting the battery exchange power with the DC bus, two new boundaries are determined for the output power of the AC grid. Obviously, exchange power with the AC grid is limited within limitation of AC/DC converter:

$$P_{\mathrm{AGmin}} \le P_{\mathrm{AG}}(t) \le P_{\mathrm{AGmax}} \tag{10}$$

The power limitation of the AC grid concerning (7) and (8) would be:

$$P_{\mathrm{min-AG}} = \max(-P_{\mathrm{bmin}} - P_{\mathrm{w}}(t) - P_{\mathrm{pv}}(t) + P_{\mathrm{l}}(t), P_{\mathrm{AGmin}}) \tag{11}$$

$$P_{\mathrm{max-AG}} = \min(-P_{\mathrm{bmax}} - P_{\mathrm{w}}(t) - P_{\mathrm{pv}}(t) + P_{\mathrm{l}}(t), P_{\mathrm{AGmax}}) \tag{12}$$

$$P_{\mathrm{min-AG}} \le P_{\mathrm{AG}}(t) \le P_{\mathrm{max-AG}} \tag{13}$$

Two boundary constraints are introduced by (13) for each hour of optimization.

4) The state of charge of the battery has to within its limits. According to the power flows shown in Fig. 1, this constraint can be defined as following:

$$E_{\mathrm{b}} \cdot (1 - DOD) \le E_{\mathrm{b0}} - \sum_{t=1}^{T} P_{b-\mathrm{in}}(t) \le E_{\mathrm{b}} \tag{14}$$

Output power of the battery including charging and discharging efficiencies can be determined:

$$P_{\mathrm{b-in}}(t) = \begin{cases} \left(-P_{\mathrm{Renew}}(t) + P_{\mathrm{l}}(t) - P_{\mathrm{AG}}(t)\right) / \eta_{\mathrm{dis}} & P_{\mathrm{b}} \ge 0 \\ \left(-P_{\mathrm{Renew}}(t) + P_{\mathrm{l}}(t) - P_{\mathrm{AG}}(t)\right) \cdot \eta_{\mathrm{ch}} & P_{\mathrm{b}} < 0 \end{cases} \tag{15}$$

Two inequality constraints at each hour are introduced to the objective function of the optimization (1) by limiting charging status of the battery storage.

C. Reserve Allocation

Definite amounts of positive and negative reserves are allocated in the battery to manage uncertainty of generation-load from renewable sources as well as load demands [15]. Positive reserve is an amount of stored energy in the battery which can be used to compensate lack of generation to balance load-generation in the online operation. Negative reserve refers to amount of free capacity of the battery which can be used to store excess power to balance load-generation in the online operation. Therefore, E_{Res} is defined as follow:

$$E_{\mathrm{Res}} = \left|\Delta P_{\mathrm{Renew}}\right| \cdot \Delta T_{\mathrm{Res}} + \left|\Delta P_{l}\right| \cdot \Delta T_{\mathrm{Res}} \tag{16}$$

© 2016, IJERMT All Rights Reserved

Uncertainty of generation in the term of maximum positive and negative deviation of forecasted power from the actual output power is known. The required time that both positive and negative reserves have to be available can be changed. Amount of the allocated reserves can be optimized based on the following factors:

- Cost of allocation of the reserves
- Avoided cost of using electricity from the main grid in a long term operation based on historical operation data of the wind-solar sources and loads in building

A trade-off between cost and benefit of allocating the reserves can lead to determination of optimal size.

Using allocated storage capacity for one reserve, increases capacity for the other reserve at the same time. For example, if positive reserve is used partly in an hour, for the next hour the system has less positive reserve but negative reserve increases equal to the amount of used positive reserve of previous hour. The same interpretation applies for using negative reserve. By allocating the positive and negative reserves, SOC constraint (14) can be rewritten as follows:

$$E_{\mathrm{b}} \cdot (1 - DOD) + E_{\mathrm{Res}} \leq E_{\mathrm{b0}} - \sum_{t=1}^{T} P_{\mathrm{b-in}}(t) \leq E_{\mathrm{b}} - E_{\mathrm{Res}} \quad (17)$$

The capacity allocation of the battery storage is shown in Fig. 2.

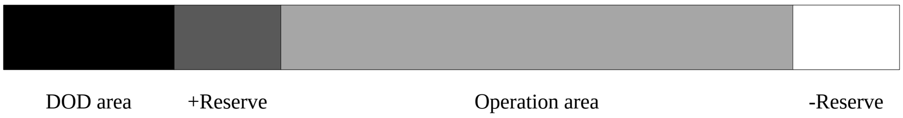

Fig. 2 Concept of storage allocation for optimized scheduling and handling generation and load uncertainties [15]

It is not permitted to run battery in the DOD area even if the allocated reserves are not enough. In such a case, regulation of the main grid or Demand System Management (DSM) would be possible solutions.

To control voltage of the DC bus in transient incidents, such as short-term voltage sag and swell, a determined storage capacity in the battery can be allocated. The battery interface can be designed in a way that receives a voltage signal from the DC bus and in those incidents it injects or absorbs active power. Motor starting in building can be an example for such a case. By allocating a determined amount of storage capacity for voltage control of the DC bus, installation cost of the storage system increases.

V. COORDINATED DROOP CONTROL OF DC MICROGRID

In this paper, in order to provide an efficient solution for integration of renewable energy sources, a control scheme applied for DC grids aims to achieve the objectives as follows [16].

- Stabilizing DC voltage during transients as well as long-term operation for different severe situations;
- Each distributed generation block operates without requirement of exchanging information with other blocks;
- It is not required to reconfigure the control scheme to keep the DC grid working normally when connecting or disconnecting of electric device blocks. It is important to get this requirement in order to fulfil a plug-and-play solution.
- Providing high power quality;
- Capturing maximum generated power from RES.

To achieve the mentioned control objectives, a coordinated droop control scheme is presented in this subsection. Wind and solar sources will follow a MPPT method in order to harvest maximum clean power from RES. BESS and AC grid will be responsible for DC voltage of the microgrid.

A. Control System of WECS and PV system

There are two control schemes for PMSG: speed controller and pitch angle controller [16]. The speed control is used to force the generator follow the predefined speed curve. The pitch angel control is aimed to prevent the generator from exceeding its rated power. When the wind speed is lower than its rated speed, the maximum power coefficient is maintained to capture maximum energy from wind. When the wind speed is high, the power coefficient is reduced by increasing the blade pitch angle to extract the maximum output power. Detail of this control is presented in [16].

For PV system, an MPPT method as presented in [16] is applied in this study.

B. Coordinated Droop Control for BESS and AC grid

BESS and AC grid are operated in DC voltage droop control as depicted in Fig. 3(b). In the voltage range from $V_{\mathrm{dc,b-}}$ to $V_{\mathrm{dc,b+}}$, BESS is responsible for controlling dc voltage. By operating that, WECS with BESS can generate flatten power to AC grid. In the voltage range from $V_{\mathrm{dc,b+}}$ to $V_{\mathrm{dc,max}}$ and also from $V_{\mathrm{dc,b-}}$ to $V_{\mathrm{dc,min}}$, the droop curve of BESS is in saturation stage, thus the BESS supports at its maximum and constant. In addition, the dc/ac converter connecting to AC grid is stabilizing dc voltage when dc voltage in the range from $V_{\mathrm{dc,G+}}$ to $V_{\mathrm{dc,max}}$ and from $V_{\mathrm{dc,G-}}$ to $V_{\mathrm{dc,min}}$. It is noticed that these values of $V_{\mathrm{dc,G}}$, $V_{\mathrm{dc,b}}$ can be adjusted. The boundaries of $I_{B,max}$, $I_{B,min}$, $I_{G,max}$ and $I_{G,min}$ must respect the capacity of the respective converters.

In the unexpected disturbances in the AC grid, the AC grid is disconnected. Then, only BESS is responsible for controlling dc voltage. The control of the BESS converter is also described as discussed above. In accordance with this control scheme, generated power from WECS is stored in BESS within its capacity.

In Fig. 3(b), $I_{cor,b}$ and $I_{cor,AG}$ is corrective signals that are used for power allocation adjustments between BESS and AC grid. Here, $I_{d,b}$ is the signal taken from the DC droop control scheme, then it is summed up with the corrective signal $I_{cor,b}$. This signal is then sent through a current control loop to control BESS. The signal $I_{d,AG}$ is also taken from the DC droop scheme, then it is adjusted by summing up with the corrective signal $I_{cor,AG}$. $I_{d,AG}$ is then sent to a PI controller in the current control loop to control ac/dc converter connecting to AC grid.

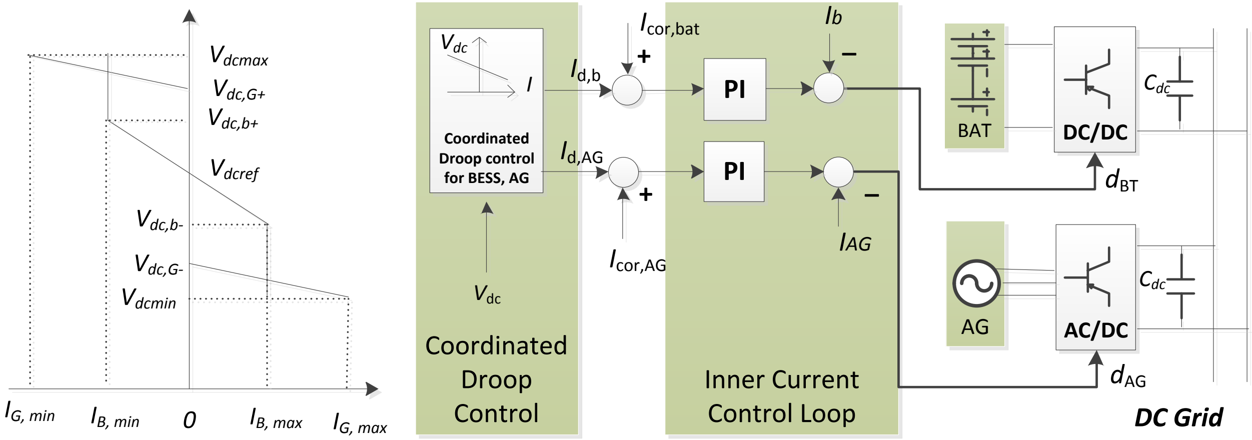

Fig. 3 (a) Coordinated droop control for BESS and AC grid; (b) Control diagram of BESS and AG units

VI. SIMULATION RESULTS

In this study, the presented long-term operation strategy is implemented by simulation in Matlab. The real time control is realized in PSCAD/EMTDC. In this study system as shown in Figure 1, the AC/DC converter connecting with AC grid and the DC/DC converter connecting to BESS are responsible for controlling DC voltage at DC bus according to the coordinated dc voltage droop control, the control system of the wind and solar sources is operated within the MPPT method to harvest maximal-clean energy from wind.

A. Long-term operation strategy

In order to simulate the dc urban microgrid, it is assumed that the system is composed of the following generations: Wind turbines having 100kW power are installed. The power of solar panels is 50 kW. The power of battery is 200 kW and the energy capacity is 500 kWh. The charge and discharge efficiencies are assumed 90% and 80% respectively. The depth of discharge is 80%. Because of uncertainties of wind and solar generations, positive and negative reserves are allocated in the battery. It is assumed that wind and solar generation forecasts have deviations of 20% of installed capacity from the predicted wind and solar power outputs. Therefore, the positive and negative reserve capacities will be 50 kWh including 40 kWh and 10 kWh for wind generation uncertainty and solar generation uncertainty respectively. Summary of the system is shown in Table 1.

Table 1. Summary of the main components

Components	Main parameters
Wind Turbines	200 kW
Solar Panels	50 kW
Battery storage	500 kWh, 200 kW: Reserve 50 kWh; DOD: 100 kWh; operating capacity: 300 kWh
Load	Peak power: 204 kVA; power factor: 0.85

The typical load of buildings in Vietnam is used as the load of the dc microgrid. The peak power of load is assumed 204 kVA and the power factor is 0.85. In the assumed buildings, the renewable generation is shown in Fig. 4. An Average wind generation power is around 50 kW (25% of installed capacity) and a peak solar generation power approximately reaches 25 kW (50% of installed capacity). It is also assumed that defined prices for buying electricity during low demand hour and high demand hour are 0.08 USD/kWh and 0.15 USD/kWh respectively.

In order to realize the presented operation strategy of the dc microgrid with objective of "net-zero energy' building, two scenarios are simulated. The first scenario is that the load is supplied by renewable energy and AC grid. In this case, no optimization is performed. The second scenario is that renewable energy and BESS together with AC grid supply the load demand. The optimization is implemented to minimum operational cost and "net-zero energy" building. After simulation, electricity consumption from grid, usage of excess renewable energy, and operational cost in two cases are compared. As a result, the benefits of the battery storage system will be determined.

© 2016, IJERMT All Rights Reserved

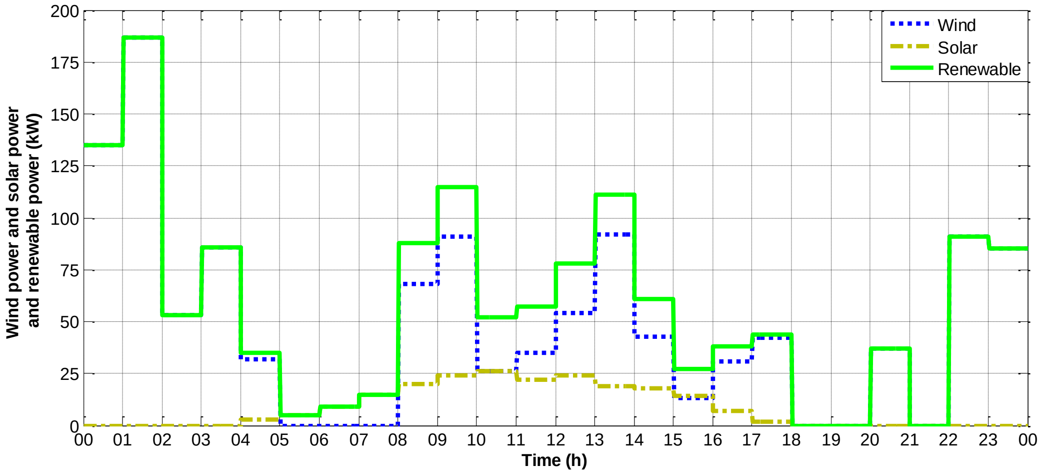

Fig. 4 Predicted renewable energy generation of a day

Considering the forecasted renewable generation profile of Fig. 4 and load demand shown in Fig. 5, simulation results for the first scenario are shown in Fig. 5. As shown in Fig. 5, the AC grid must supply load almost the day, especially during high demand hours. With the optimized operation, simulation results are shown in Fig. 6. It seen that with the help of BESS, clean energy from wind and solar sources can be utilized and reduction of electricity from the AC grid during high demand hours can be achieved. The dc microgrid with this operational method can supply load all day. It realizes the concept of a "Net-zero energy building".

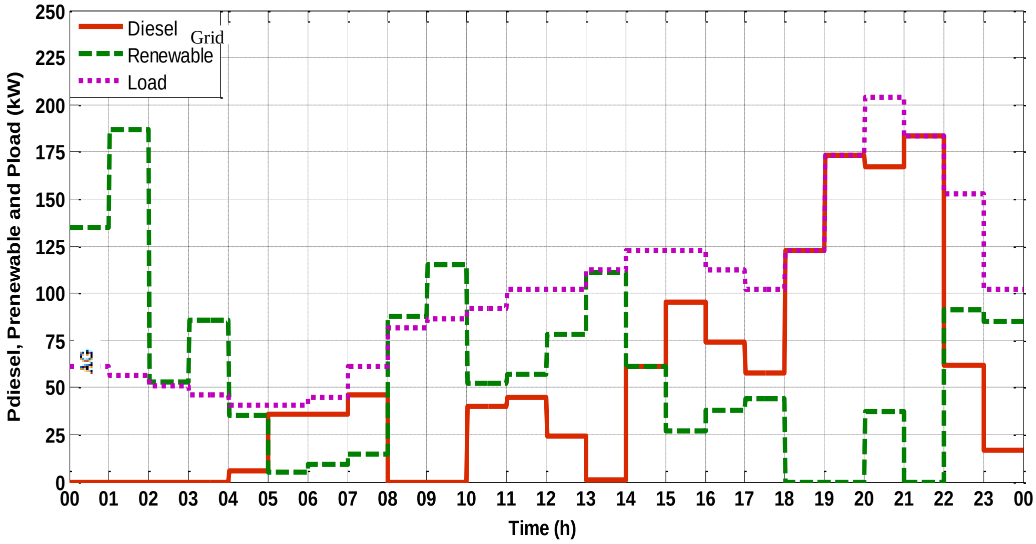

Fig. 5 The first scenario: Operation of the microgrid without battery

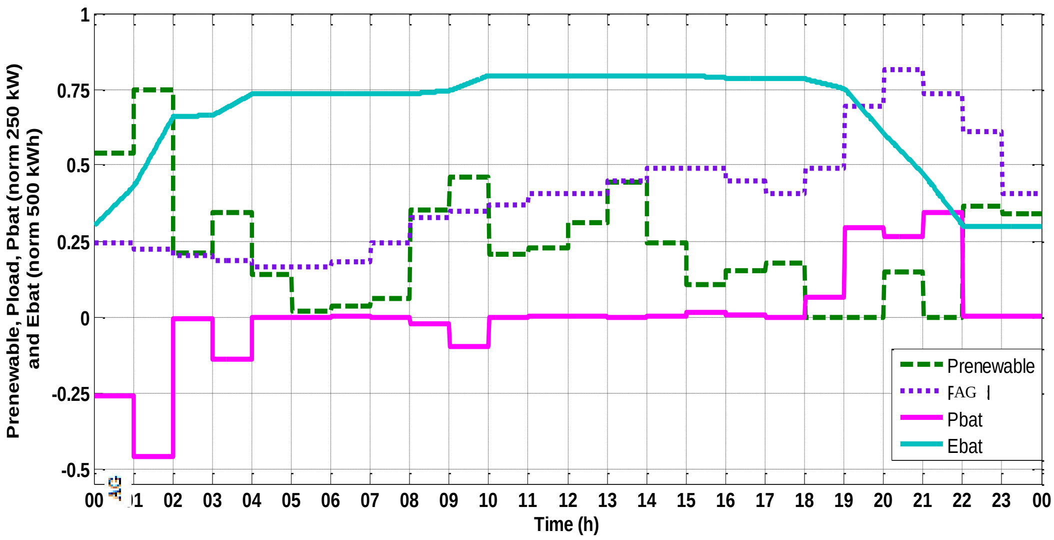

Fig. 5 The first scenario: Optimization of the microgrid with battery

B. Real-time control

The dc building microgrid integrated with distributed generations and battery shown in Figure 1, as in interconnected mode, is simulated. The dc droop control is used to stabilize dc voltages. The parameters of this case are listed in Appendix. The input includes the wind speed V_W, the voltage source and inner resistance of the Thevenin equivalent circuit of PV array V_{thar}, R_{thar}; and the load. The wind speed changes from 12m/s to 14m/s at t = 1s; the voltage source of PV array changes from 692V to 678V and the inner resistance from 2.4 Ω to 2.9Ω at t = 3s; and the load changes from 55kW to 45kW at t = 5s.

The transients of the nodal voltages will be observed in Figure 6(b) when the inputs change. Verification of the model in PSCAD and Matlab is shown in Figure 6(a). The power of distributed generations is depicted in Figure 6(c). It is seen that during small changes, BESS can control dc voltage without the help of AC grid.

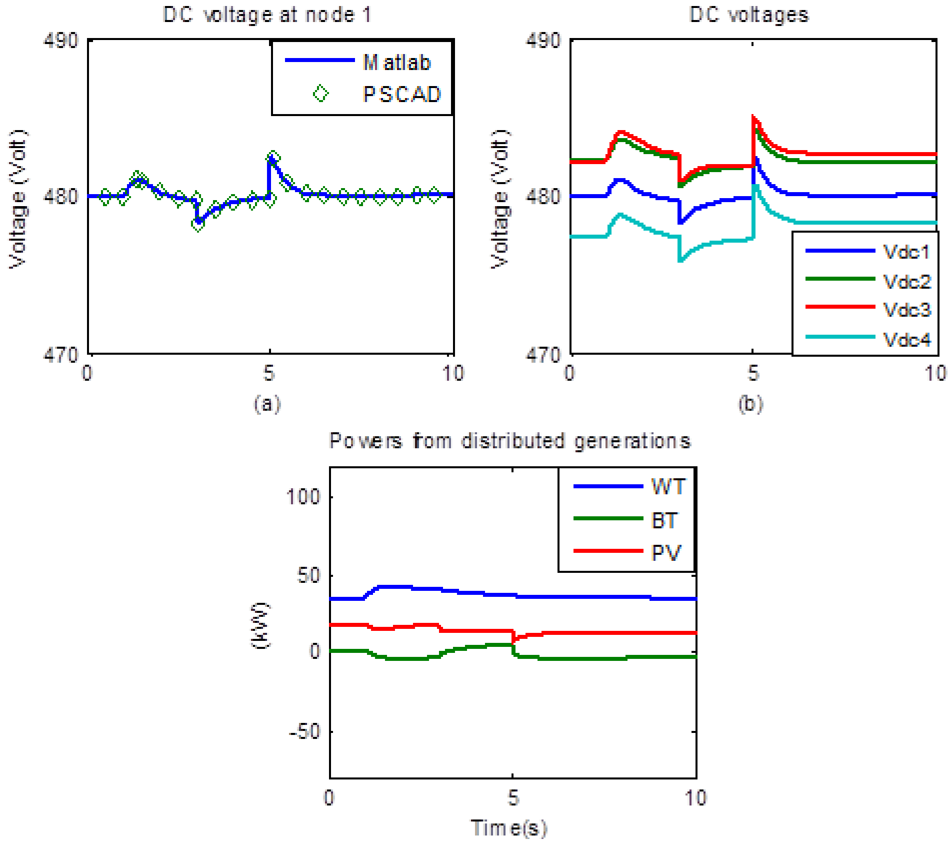

(d)(c)

Fig. 6: Transient of the microgrid with changes from wind speed; solar irradiation and load

VII. CONCLUSIONS

A concept of a dc ring microgrid for wind and solar integration in a so-call net-zero energy buildings has been presented. The optimized operation strategy is introduced to minimize cost and emissions as a result of minimal usage of electricity from the main grid. The control employed for WECS and PV track on maximum available wind and solar power dynamically. The coordinated droop control applied for BESS and AC grid to control dc voltage at dc bus. This control scheme facilitates integration of distributed generation sources. Thanks to the presented method, optimal usage of clean energy can be achieved, thus reduce operation cost as well as emissions.

APPENDIX: PARAMETERS FOR SIMULATION

Notation	Value	Notation	Value	Notation	Value
		DC Grid block			
R_{12}	0.064 Ω	L_{12}	0.255mH	C_{12}	10.7 nF
R_{23}	0.064 Ω	L_{23}	0.255mH	C_{23}	10.7 nF
R_{34}	0.064 Ω	L_{34}	0.255mH	C_{34}	10.7 nF
R_{41}	0.064 Ω	L_{41}	0.255mH	C_{42}	10.7 nF
		PV System			
L_{ddPV}	1 mH	C_{dcPV}	5mF	K_{PV}	0.01/V
V_{dcref}	480 V				
		Wind Energy Conversion System			
R_t	5 m/s	ρ	1.205 kg/m3	V_{wrated}	12 m/s

K_{popt}	7.877 W/(rad/s)3	C_{pmax}	0.4412	$P_{genrated}$	36 kW
ω_{rrated}	16.6 rad/s	p	2	H	0.05 sec
Ψ_f	90 Wb	L_{md}	0.334 H	L_{mq}	0.217 H
L_{ls}	0.0344 H	R_s	0.08 Ω	K_{p1}	1.01/A
K_{i1}	2.21/A.s	K_{p2a}	5 A/rad	K_{i2a}	150 A/rad.s
K_{p2b}	1.01/A	K_{i2b}	2.21/A.s	K_{p3}	2 deg/rad
K_{i3}	4 deg/rad.s	C_{dcWT}	5 mF		
Battery Energy Storage System					
L_{ddBT}	120 mH	C_{dcBT}	5 mH	R_{1BT}	0.1 Ω
R_{2BT}	0.075 Ω	R_{pBT}	25.10^6Ω	C_{1BT}	500 F
C_{bBT}	300 (F)	K_{p4aBT}	1 A/V	K_{i4aBT}	5 A/V.s
K_{p4bBT}	0.3/A	K_{i4bBT}	2/A.s	V_{dcref}	480 V
AC grid					
R_s	0.1 Ω	L_s	2.7 mH	E_s	6 kV
K_{pa}	3	K_{pb}	0.01	C_{dcAG}	3000F
K_{ib1}	0.2				

REFERENCES

[1] F. Giraud and Z. M. Salameh, “Steady-state performance of a grid-connected rooftop hybrid wind-photovoltaic power system with battery storage,” IEEE Trans. Energy Convers., vol. 16, no. 1, pp. 1–7, Mar. 2001.

[2] B. S. Borowy and Z. M. Salameh, “Methodology for optimally sizing the combination of a battery bank and PV array in a wind/PV hybrid system,” IEEE Trans. Energy Convers., vol. 11, no. 2, pp. 367–375, Mar. 1996.

[3] M. Cheng, S. Kato, H. Sumitani, and R. Shimada, “Flywheel-based AC cache power for stand-alone power systems,”IEEJ Trans. Electr. Electron. Eng., vol. 8, no. 3, pp. 290–296, May 2013.

[4] H. Louie and K. Strunz, “Superconducting magnetic energy storage (SMES) for energy cache control in modular distributed hydrogen-electric energy systems,”IEEE Trans. Appl. Supercond., vol. 17, no. 2, pp. 2361–2364, Jun. 2007.

[5] A. L. Dimeas and N. D. Hatziargyriou, “Operation of a multiagent system for microgrid control,”IEEE Trans. Power Syst., vol. 20, no. 3, pp. 1447–1455, Aug. 2005.

[6] F. Katiraei and M. R. Iravani, “Power management strategies for a microgrid with multiple distributed generation units,” IEEE Trans. Power Syst., vol. 21, no. 4, pp. 1821–1831, Nov. 2006.

[7] A. G. Madureira and J. A. Pecas Lopes, “Coordinated voltage support in distribution networks with distributed generation and microgrids,”IET Renew. Power Generat., vol. 3, no. 4, pp. 439–454, Dec. 2009.

[8] M. H. Nehrir, C. Wang, K. Strunz, H. Aki, R. Ramakumar, J. Bing, et al., “A review of hybrid renewable/alternative energy systems for electric power generation: Configurations, control, and applications,” IEEE Trans. Sustain. Energy, vol. 2, no. 4, pp. 392–403, Oct. 2011.

[9] R. Majumder, B. Chaudhuri, A. Ghosh, R. Majumder, G. Ledwich, and F. Zare, “Improvement of stability and load sharing in an autonomous microgrid using supplementary droop control loop,”IEEE Trans. Power Syst., vol. 25, no. 2, pp. 796–808, May 2010.

[10] D. Westermann, S. Nicolai, and P. Bretschneider, “Energy manage-ment for distribution networks with storage systems—A hierarchical approach,” inProc. IEEE PES General Meeting, Convers. Del. Electr. Energy 21st Century, Pittsburgh, PA, USA, Jul. 2008.

[11] D. Nguyen Huu, “Adaptive coordinated droop control for multi-battery storage,” IEEE Conf. Eurocon 2015, Spain, 2015.

[12] H. Kakigano, Y. Miura, and T. Ise, “Low-voltage bipolar-type DC microgrid for super high quality distribution,”IEEE Trans. Power Electron., vol. 25, no. 12, pp. 3066–3075, Dec. 2010.

[13] D. Chen, L. Xu, and L. Yao, “DC voltage variation based autonomous control of DC microgrids,” IEEE Trans. Power Del., vol. 28, no. 2, pp. 637–648, Apr. 2013.

[14] L. Roggia, L. Schuch, J. E. Baggio, C. Rech, and J. R. Pinheiro, “Integrated full-bridge-forward DC-DC converter for a residential microgrid application,”IEEE Trans. Power Electron., vol. 28, no. 4, pp. 1728–1740, Apr. 2013.

[15] K. Strunz, E. Abbasi, D. Nguyen Huu,“ DC Microgrid for wind and solar power integration,“ IEEE Journal of Emerging and Selected Topics in Power Electronics, vol. 2, Issue 1, page(s): 115-126, 2014.

[16] D. Nguyen Huu, Ph.D. thesis: “State-Space Modelling and Voltage Control of AC-DC Networks,” Technical University of Berlin, 2014.

© 2016, IJERMT All Rights Reserved